Experimental Trial

Targeted Nanoparticles that Mimic Immune Cells in Pain Control Inducing Analgesic and Anti-inflammatory Actions: A Potential Novel Treatment of Acute and Chronic Pain Conditions

Susan Hua, PhD[1], and Peter J. Cabot, PhD[2]

From: [1]The University of Newcastle, Newcastle, Australia; and [2]The University of Queensland, Brisbane, Australia

Address Correspondence:
Susan Hua, PhD
The University of Newcastle
School of Biomedical Sciences and Pharmacy
Susan.Hua@newcastle.edu.au

Disclaimer: The authors wish to thank the National Health and Medical Research Council (NHMRC), The University of Newcastle, and The Pharmacy Research Trust of New South Wales for providing financial support for our research . Conflict of interest: None.

Manuscript received: 09-05-2012
Revised manuscript received 10-29-2012
Accepted for publication: 01-18-2013

Free full manuscript: www.painphysicianjournal.com

Background: The peripheral immune-derived opioid analgesic pathway has been well established as a novel target in the clinical pain management of a number of painful pathologies, including acute inflammatory pain, neuropathic pain, and rheumatoid arthritis.

Objective: Our objective was to engineer targeted nanoparticles that mimic immune cells in peripheral pain control to deliver opioids, in particular loperamide HCl, specifically to peripheral opioid receptors to induce analgesic and anti-inflammatory actions for use in painful inflammatory conditions. This peripheral analgesic system is devoid of central opioid mediated side effects (e.g., respiratory depression, sedation, dependence, tolerance).

Study Design: A randomized, double blind, controlled animal trial.

Methods: Thirty-six adult male Wistar rats (200 - 250 g) were randomly divided into 6 groups: loperamide HCl-encapsulated anti-ICAM-1 immunoliposomes, naloxone methiodide + loperamide HCl-encapsulated anti-ICAM-1 immunoliposomes, loperamide HCl-encapsulated liposomes, empty anti-ICAM-1 immunoliposomes, empty liposomes, and loperamide solution. Animals received an intraplantar injection of 150 μL Complete Freund's Adjuvant (CFA) into the right hindpaw and experiments were performed 5 days post-CFA injection, which corresponded to the peak inflammatory response. All formulations were administered intravenously via tail vein injection. The dose administered was 200 μL, which equated to 0.8 mg of loperamide HCl for the loperamide HCl treatment groups (sub-therapeutic dose). Naloxone methiodide (1 mg/kg) was administered via intraplantar injection, 15 minutes prior to loperamide-encapsulated anti-ICAM-1 immunoliposomes. An investigator blinded to the treatment administered assessed the time course of the antinociceptive and anti-inflammatory effects using a paw pressure analgesiometer and plethysmometer, respectively. Biodistribution studies were performed 5 days post-CFA injection with anti-ICAM-1 immunoliposomes and control liposomes via tail vein injection using liquid scintillation counting (LSC).

Results: Administration of liposomes loaded with loperamide HCl, and conjugated with antibody to intercellular adhesion molecule-1 (anti-ICAM-1), exerted analgesic and anti-inflammatory effects exclusively in peripheral painful inflamed tissue. These targeted nanoparticles produced highly significant analgesic and anti-inflammatory effects over the 48 hour time course studied following intravenous administration in rats with Complete Freund's Adjuvant-induced inflammation of the paw. All control groups showed no significant antinociceptive or anti-inflammatory effects. Our biodistribution study demonstrated specific localization of the targeted nanoparticles to peripheral inflammatory tissue and no significant uptake into the brain.

Limitations: In vivo studies were performed in the well-established rodent model of acute inflammatory pain. We are currently studying this approach in chronic pain models known to have clinical activation of the peripheral immune-derived opioid response.

Conclusions: The study presents a novel approach of opioid delivery specifically to injured tissues for pain control. The study also highlights a novel anti-inflammatory role for peripheral opioid targeting, which is of clinical relevance. The potential also exists for the modification of these targeted nanoparticles with other therapeutic compounds for use in other painful conditions.

Key words: Pain, inflammation; immune cells, opioids, ICAM-1, loperamide, targeted drug delivery, immunoliposomes

Pain is a major health problem having a significant impact not just on sufferers, but also on the broader community and economy. Painful pathologies such as neuropathic pain and arthritis and musculoskeletal conditions are highly prevalent and large contributors to illness, pain, and disability. Despite the wide-ranging conditions and symptoms, the main subgroups share a significant underlying inflammatory component, and are limited by effective and safe clinical management options (1,2). The peripheral immune-derived opioid analgesic pathway has been well established as a novel target in the clinical pain management of these conditions (1). In particular at early stages of inflammation, both peripheral and central opioid receptors are involved in antinociceptive effects, whereas at later stages endogenous analgesia is mediated exclusively by peripheral opioid receptors (3). Therefore, peripheral opioid mechanisms of pain control become more prevalent with the duration and severity of inflammation (3). In the periphery, endogenous analgesia is elicited by immune cells entering inflamed tissue and releasing opioid peptides that activate up-regulated opioid receptors on sensory nerve terminals (1) (Fig. 1). Inflammation has been shown to increase the expression of opioid peptides within these immune cells (4). All opioid peptides as well as their mRNA transcripts encoding their precursor proteins have been identified within immune cells, with β-endorphin being the most prominent (4,5).

We have previously identified a physical outcome associated with a direct interaction between the immune system and the peripheral nervous system in peripheral analgesia (6). Adhesion molecules, in particular intercellular adhesion molecule-1 (ICAM-1), have been shown to play an important role in the transmigration of opioid-containing immune cells to injured tissue, as well as the direct binding of these immune cells to sensory neurons to produce adequate analgesia (Fig. 1). Immunohistochemical studies have revealed ICAM-1 expression on both nonhaematopoietic cells (e.g.,

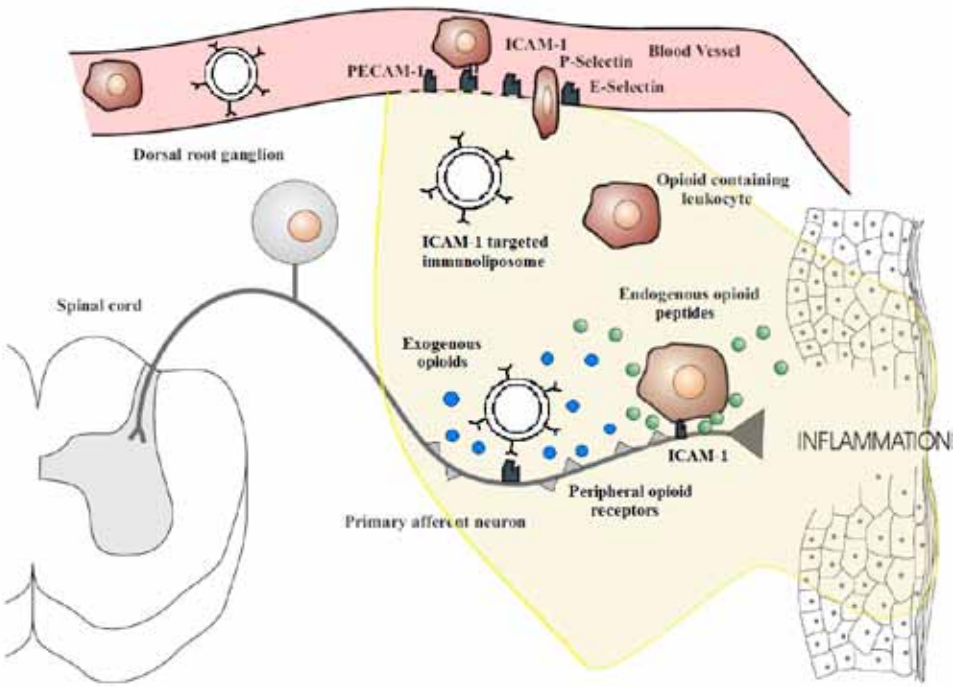

Fig. 1. *Mimicking the migration of opioid-containing immune cells and opioid secretion within inflamed tissue using targeted nanoparticles. Adhesion molecules interact with their respective ligands to facilitate endothelial transmigration of immune cells. In response to stress or releasing agents (e.g., corticotropin-releasing hormone or interleukin-1), the immune cells secrete opioid peptides. Opioid peptides or exogenous opioids bind to opioid receptors on primary afferent neurons, leading to analgesia. Direct adhesion between opioid-containing immune cells and peripheral sensory neurons may be necessary to release opioid peptides within the effective range of peripheral opioid receptors. The immune cells, depleted of opioids, then migrate to regional lymph nodes.*

vascular endothelium) as well as haematopoietic cells (e.g., leukocytes and macrophages). Although ICAM-1 expression is low in both nonhaematopoietic cells and resting peripheral blood leukocytes, it is upregulated by cytokines [e.g., tumor necrosis factor-alpha (TNF-α), interleukin-1 (IL-1)] and in activated T- and B- lymphocytes, respectively (7).

To mimic the endogenous peripheral opioid analgesic response in injured tissue, we used opioid-containing immune cells as a structural platform in the design of synthetic targeted nanoparticles that have the ability to release encapsulated opioids directly at the site of inflammation. In this study the highly potent peripheral mu-opioid receptor (MOR) agonist, loperamide HCl, was incorporated in liposomes directed towards ICAM-1, to create a delivery system with the unique properties of binding to adhesion molecules that are significantly increased at the site of tissue injury. Loperamide HCl is a piperidine derivative (8) that was developed to mimic the effect of morphine on the intestinal tract as an antidiarrhoeal agent, without any central morphinomimetic effects (9). It exhibits high affinity and selectivity for peripheral mu-opioid receptors, but does not have analgesic effects when administered orally or intravenously due to its physicochemical properties (1,10-14).

The design of peripherally acting analgesics may have widespread potential for clinical use by optimizing drug concentrations at the site of injury thereby avoiding systemically active drug levels, adverse systemic effects, or drug interactions, whilst maintaining effective analgesia. The immune-cell derived opioid pathway is devoid of typical opioid mediated side effects (e.g., respiratory depression, sedation, dependence, tolerance, constipation) (15), which will have important implications for the management of chronic pain. A major advantage of targeting peripheral opioid receptors is their mechanism of action of inhibiting calcium (and possibly sodium) channels, which simply renders the nociceptor less excitable to the plethora of stimulating molecules expressed in damaged tissue. Therefore, peripherally acting opioids can prevent and reverse the action of multiple excitatory agents simultaneously (16). Therefore it may be used to produce clinically significant and effective analgesia in a range of inflammatory pain conditions. This study is the first to apply the concept of disease-site targeting to mimic the inherent opioid containing immune cell response, shown to produce both site-directed analgesic and anti-inflammatory actions.

Methods

Liposome-related Materials

1,2-distearoyl-sn-glycero-2-phosphocholine (DSPC) and 1-{8-[4(p-maleimidophenyl)butaroylamino]-3,6-dioxaloctyl}-2,3-distearyl glyceryl-dl-ether (MPB-TRIG-DSGE) were purchased from Northern Lipid (Vancouver, Canada). The CBQCA protein assay kit was from Invitrogen (Melbourne, Australia). Cholesterol, N-succinimidyl-3- (2-pyridyldithio) propionate (SPDP), and Sepharose CL-4B were from Sigma-Aldrich (Sydney, Australia). Tris(2-Carboxyethyl) phosphine Hydrochloride (TCEP) was purchased from Quantum Scientific (Queensland, Australia). Rabbit IgG antibody and anti-ICAM monoclonal antibody were obtained from Chemicon International Inc. (Melbourne, Australia). PD-10 column was from GE Healthcare Bio-Sciences Pty. Ltd. (Sydney, Australia). All other chemicals and solvents were of at least analytical grade.

Cell-related Materials

Reagents were obtained from the following sources: penicillin, streptomycin, Dulbecco's Phosphate Buffered Saline, and RPMI 1640 media were obtained from GIBCO/Life Technologies (Melbourne, Australia); fetal calf serum, collagenase (Type II), dimethylsulfoxide (DMSO), trypan blue solution 0.4%, tumor necrosis factor-alpha (TNF- α) and all buffer reagents were from Sigma-Aldrich, (Sydney, NSW, Australia); trypsin- EDTA (1:250) was from Australian Biosearch (Trace Plastics) (Perth, Australia). FITC-conjugated mouse anti-rat OX-43 monoclonal antibody was from Invitrogen (Melbourne, Australia). All other reagents were of analytical grade. The hemacytometer used for cell counts was purchased from Hausser Scientific (Horsham, PA). The fluorescent plate reader Novostar and its corresponding software (Novostar) were obtained from BMG Labtechnologies (Mt Eliza, Victoria, Australia).

Preparation of Conventional Liposomes

Conventional liposomes were prepared according to the method of dried lipid film hydration. Briefly, 16 mg DSPC and 4 mg cholesterol (molar ratio of 2:1) (and 4 mg loperamide HCl) were solubilized in 6 mL chloroform:methanol (2:1, v/v) in a 50 mL round bottomed flask and dried by rotary evaporation under reduced pressure (200 mbar; 15 min; 60°C). The resultant thin lipid film was hydrated with the addition of 1 mL of PBS (pH 7.4) and resuspended in a 65°C water bath. The resultant multilamellar dispersions were reduced

in size and lamellarity by probe sonication (60 amps; 5 min) at 65°C. Liposomes were stored at 4°C, under nitrogen gas and in the dark, and were used within 7 days.

Preparation of Immunoliposomes

Immunoliposomes were prepared according to the method of dried lipid film hydration using our novel method as previously described (17). Liposomes composed of DSPC and cholesterol (molar ratio 2:1) containing MPB-TRIG-DSGE at 1.5 mol percent of DSPC as a coupling lipid were prepared according to the method of dried lipid film hydration in PBS buffer (pH 7.4). The resulting multilamellar dispersions were reduced in size and lamellarity by ultrasonication at 60 amp for 5 minutes. The activated liposome suspension was immediately mixed with thiolated antibody at room temperature. Thiolated antibodies were prepared by conjugating anti-ICAM-1 monoclonal antibodies (25 μg) or non-specific rabbit IgG (25 μg) with a heterobifunctional reagent N-succinimidyl-3-(2-pyridyldithio) propionate (SPDP) (6.25 mg/mL; SPDP/mAb molar ratio = 10:1). Excess SPDP was removed through a PD-10 column equilibrated with distilled water. Fractions containing pyridyldithiopropionated-Ab (PDP-Ab) conjugates (assessed by absorbance in 280 nm) were pooled and lyophilized to form a solid product, which was then stored at 4°C under nitrogen gas. To produce thiolated- Ab (Ab-SH), PDP-Ab was reduced with 5 mM TCEP for 5 minutes. Absorbance was checked at 280 nm (protein concentration) and 343 nm (SPDP modification), in order to ensure stability of the compound as described above. The Ab-SH was mixed immediately with liposomes and incubated for one hour at room temperature with stirring in the dark. Unconjugated Ab was removed by size exclusion chromatography using a Sepharose CL-4B column (1cm x 16cm), which excluded liposomes in the void volume, or by TLX ultracentrifugation (Optima) (100 000 g; 45 minutes). Immunoliposomes were stored at 4°C, under nitrogen gas and in the dark, and were used within 7 days. The size distribution of the liposomal dispersion was determined by dynamic laser light scattering (Zetasizer 3000, Malvern, Worcestershire, United Kingdom). Loperamide-HCl encapsulated anti-ICAM-1 immunoliposomes had a mean particle size of 286 nm and a polydispersity index of 0.307. The size and polydispersity of the control liposome formulations were similar. Quantification of the amount of antibody associated with liposomes was determined using the CBQCA protein assay (Invitrogen) using bovine serum albumin for the preparation of the standard curve. The conjugation efficiency equated to 96% and 99% for anti-ICAM-1 immunoliposomes and rabbit IgG immunoliposomes, respectively. This procedure resulted in high loperamide HCl encapsulation efficiency of > 99%, which equated to 3.981 ± 0.078 mg/mL of loperamide HCl encapsulated in the liposome suspension. Loperamide HCl solution was prepared by dissolving 4 mg loperamide HCl in 50% DMSO/50% PBS pH 7.4.

Liposome Stability Assay

The dialysis technique was used to evaluate the *in vitro* stability of liposomes encapsulating loperamide HCl by separating the encapsulated from the non-encapsulated drug. Release properties of loperamide HCl were measured as the accumulative release percentages in an outer medium during 48 hours to compare the stability of the liposome formulations in phosphate buffered saline pH 7.4 (PBS) and 50% fetal calf serum (FCS) at 37°C. The degree of stability of the nanoparticles influences their circulation time and controlled release capability when administered intravenously. To circumvent potential solubility issues of loperamide HCl across the dialysis membrane, a modified assay was developed to assess true release of loperamide HCl from the liposomes without surpassing saturation point. In brief, 50 μl of 4 mg/mL loperamide HCl-encapsulated liposome suspension (equivalent to 200 μg loperamide HCl) was added in a dialysis bag with either PBS pH 7.4 or 50% FCS to a volume of 10 mL. The dialysis system was suspended in a release volume of 40 mL PBS at 37°C and rotated at 200 rpm. For control groups, 4 mg of loperamide HCl was dissolved in 200 mL PBS pH 7.4, and 10 mL of this solution (equivalent to 200 μg loperamide HCl) was placed in a dialysis bag and stability was assessed using the above dialysis method. At scheduled intervals, 200 μl of the release medium was collected for HPLC assay. The same volume of fresh PBS buffer at the same temperature was added immediately to maintain constant release volume. Calibration curves were established by plotting the standard concentrations of loperamide HCl dissolved in PBS pH 7.4 versus the peak height. The loperamide HCl release percentage was obtained according to: $Drug\ release\ (\%) = (D_t/D_0) \times 100\%$, where D_t and D_0 indicate the amount of drug released from the liposome suspension at certain intervals and the total amount of drug in the liposome suspension, respectively. At the end of the study, the liposome samples were recovered from the dialysis system, and lysed with ethanol for analysis for loperamide HCl content by HPLC.

Cell Culture

Primary high endothelial venule cells (HEV) were isolated and cultured from rat lymph nodes as previously described (18). In brief, male Wistar rats were sedated by inhalation of 50% O_2/50% CO_2 and sacrificed by asphyxiation with 100% CO_2. Popliteal lymph nodes were surgically collected under sterile conditions. The tissue was washed twice with Dulbecco's Phosphate Buffered Saline (D-PBS with calcium chloride and magnesium chloride) plus antibiotics (50 units/mL penicillin + 50 μg/mL streptomycin) (DAB), and then incubated in 10% betadine in DAB for 10 minutes, before being washed 3 times with DAB. The tissue was minced finely with sharp-bladed scissors to dissociate the cells and allowed to settle out of 20 mL DAB for 1 – 2 minutes. The cell-rich supernatant was discarded, and the tissue was washed 3 times with DAB, before being resuspended at 50 mg/mL in RPMI 1640 containing 10mM-$NaHCO_3$, 20mM-HEPES, 2mM-glutamine, antibiotics ($RPMI_{Inc}$) and 0.5% type II collagenase. After shaking for 60 minutes at 37°C, the tissue was dispersed with a Pasteur pipette, resuspended in 10mL $RPMI_{Inc}$ and the cells were dissociated through a 100 μm nylon mesh supported in 23 mm Millipore Swinnex filter holder. Isolated cells were collected by centrifugation at 250 g for 5 minutes and then plated in a tissue culture flask containing complete medium (RPMI 1640 containing 20mM-$NaHCO_3$ and 2 mM-glutamine, 20% heat-inactivated (56°C; 30 min) fetal calf serum, 100 IU/mL penicillin and 100 μg/mL streptomycin). Cell were cultured in incubators maintained at 37°C in a humidified atmosphere of 5% CO_2 in air. Feeding media was routinely replaced every 48 – 72 hours. HEV cells were identified by FITC-conjugated OX-43 labeling under fluorescence microscopy, and further supported by ICAM-1 labeling. Viability and morphology of the cells were monitored by phase contrast microscopy and consistently found to be unchanged throughout the experiments. Viable cells were counted using the Trypan Blue Exclusion method and a haemocytometer.

Specificity of Binding to ICAM-1 on HEV Cells

HEV cells were seeded in 96-well tissue culture plates at $4x10^4$ cells per well in complete medium (RPMI 1640 containing 20mM-$NaHCO_3$ and 2mM-glutamine, 20% heat-inactivated (56°C; 30 minutes) fetal calf serum, 100 IU/mL penicillin and 100 μg/mL streptomycin) and activated with TNF-α (1 ng/mL) for 24 hours at 37°C in 5% CO_2. The fluorescent dye DiI was incorporated into the phospholipid bilayer as a marker for the liposomes. Following activation, liposomes were added to the wells and the cultures incubated for 2 hours at 4°C or 5 hours at 37°C. Binding was assessed in vitro after 2 h of incubation at 4°C to determine exclusively cell binding, or after 5 hours of incubation at 37°C to determine cell association. After washing cells to remove unbound liposomes, binding was then assessed via fluorimetric detection to assess exclusively cell binding at excitation/emission wavelengths corresponding to DiI (549nm/565nm) (POLARstar OPTIMA fluorescent microplate reader; BMG LABTECH Pty. Ltd.,Victoria, Australia). Background reading was assessed with cells incubated in medium alone.

Cellular Uptake of Liposomes

To evaluate cell association of ICAM-1 targeted immunoliposomes, HEV cells were plated in 96-well tissue culture plates at an initial density of $4x10^4$ cells per well and grown until confluent under the conditions described above. Before experiments, cell monolayers were activated with TNF-α (1 ng/mL) for 24 hours at 37°C. After an exchange of the medium, cells were then incubated in serum-free medium containing fluorescent labeled liposomes for 2 hours at 4°C or 5 hours at 37°C. Two temperatures were used in order to differentiate receptor binding and internalization. At 4°C, it was expected that no receptor internalization occurred, whereas both receptor binding and internalization took place at 37°C (19,20). At the end of incubation, the cells were washed 3 times with ice-cold PBS before fluorimetric detection to assess extracellularly bound liposomes (Polarstar, BMG). Surface-bound fluorescence was released by acid wash (10 minutes 0.1M HCl) (21) before lysis of the cells with addition of 1% Triton-X100 in PBS for 10 minutes at 37°C. Results retrieved by acid wash were expressed as extracellularly bound fluorescence, whereas fluorescence in the lysis fractions was expressed as internalized fluorescence. Background reading was assessed with solubilized cells without prior incubation with liposomes.

Animals and Induction of Inflammation

Male Wistar rats (200 - 250 g) (ARC, Australia) were anaesthetised by a brief exposure to 2% isoflurane (Abbot, Cronulla, Australia) and received an intraplantar injection of 150 μl Complete Freund's Adjuvant (CFA) (Sigma–Aldrich, Sydney, Australia) into the right hindpaw. Animals were housed in groups of 2 or 3 per cage, under 12 h light-dark cycles in a room with controlled temperature (22°C) and humidity (60%). Rats had free

access to standard rodent chow and water, and were used after a minimum of 5 days acclimatization to the housing conditions. All animal experiments were performed with permission from the Animal Experimentation and Ethics Committee at The University of Queensland and The University of Newcastle.

Assessment of Antinociception and Inflammation

Baseline measurements of paw pressure threshold (PPT) and paw volume were obtained prior to CFA injection. On the basis of previous studies, experiments were performed 5 days post-CFA injection, which corresponded to the peak inflammatory response. Baseline measurements were again assessed 5 days following CFA injection before intravenous administration of loperamide HCl-encapsulated anti-ICAM-1 immunoliposomes or control liposome formulations via tail vein injection. The dose administered was 200 μl, which equated to 0.8 mg of loperamide HCl for the loperamide HCl treatment groups. Naloxone methiodide (1mg/kg) was administered via intraplantar injection, 15 minutes prior to loperamide-encapsulated anti-ICAM-1 immunoliposomes. An investigator blinded to the treatment administered assessed the time course of the antinociceptive and anti-inflammatory effects. Inflammation was assessed with a rat plethysmometer (Ugo Basile, Comerio, Italy). This involves the placement of each paw into the displacement cell and the instrument measures displacement and interprets this as volume. Nociceptive thresholds were assessed using the paw pressure analgesiometer (Ugo Basile, Comerio, Italy), which involves a sliding weight scale and a blunt probe that places pressure on the paw against a plate surface. Animals respond by flinching or moving the paw. Cut-offs were set at 250 g for pressure threshold, which correspond to the maximum ethical load. PPTs were assessed at baseline, 15 minutes, 1 hour, 2 hours, 4 hours, 7 hours, 10 hours, 24 hours, and 48 hours. Paw volumes were evaluated at baseline, 24 hours, and 48 hours. During the experiments, the sequence of inflamed and non-inflamed paw testing was alternated to preclude order effects for PPT, and triplicate values were averaged.

Biodistribution Study

Biodistribution studies were performed 5 days post-CFA injection with anti-ICAM-1 immunoliposomes and control liposomes via tail vein injection using liquid scintillation counting (LSC). Liposomes were radiolabelled with [^{3}H]-CHE (PerkinElmer) with loperamide HCl loading at a specific ratio of 0.5 μci/μmol phospholipid. The use of [^{3}H]-CHE is convenient for these studies because it is a stable, nonexchangeable, and nondegradable marker of liposomes, thus providing an estimate of the cumulative liposome dose in tissue. The dose administered was 200 μl, which equated to 0.8 mg of loperamide HCl and 7.41 x 10^4 Bq. Biodistribution was assessed 7 hours after liposome injection, which corresponded to peak antinociceptive effect of loperamide HCl-encapsulated anti-ICAM-1 immunoliposomes. At the scheduled time point, rats were sacrificed by asphyxiation with 100% CO_2 and cervical dislocation. Paw tissues, brain, liver, and kidneys were removed, rinsed in physiological saline, and frozen at –20°C until further processing. Tissue samples were weighed into scintillation vials and prepared as per protocol described by PerkinElmer (22). Radioactivity was measured in terms of number of disintegrations per minute (DPM) of [^{3}H]-CHE of each tissue sample. The amount of radioactivity was then expressed as the number of Bq per gram of tissue using the following conversion: 1 Bq = 60 DPM.

Statistical Analyses

All data are expressed as means ± standard error of the mean (SEM). Comparisons were made using the Mann-Whitney U test to assess non-parametric independent data. The one-way analysis of variance (ANOVA) was used to evaluate parametric data. Differences were considered significant when $P < 0.05$.

Results

Stability of Liposomal Formulations Entrapping Loperamide HCl

In order to circumvent potential solubility issues of loperamide HCl across the dialysis membrane, an assay was developed to assess the true release of loperamide HCl from the liposomes without surpassing the saturation point. At a dilution of 200 μg of loperamide HCl in 40 mL of PBS release volume, which equated to 200 μg of loperamide HCl in 10 mL of PBS within the dialysis tubing, minimal release was observed in both PBS and 50% FCS at 37°C (Fig. 2A). The stability of the liposome formulation was slightly lower in 50% serum in comparison to PBS due to the bioactive substance in FCS, however the difference was not significant. The diffusion of free drug through the dialysis membrane was also investigated with 100% of loperamide HCl solution being recovered in the dialysis medium within 6 hours as determined by HPLC, demonstrating that the release

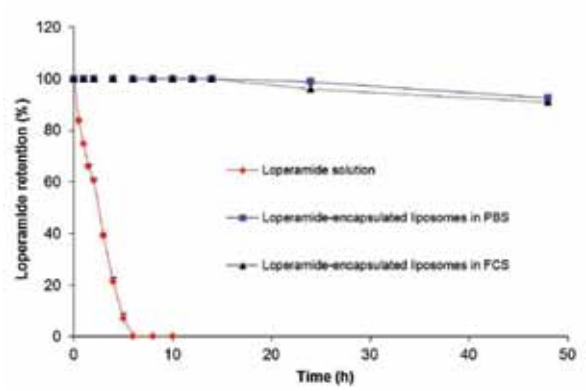

A

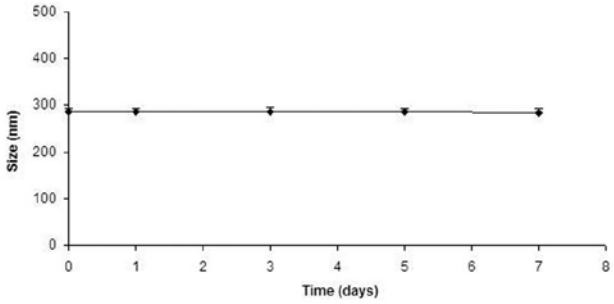

B

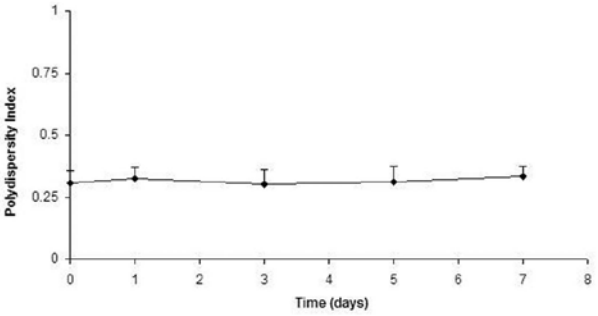

C

Fig. 2. *Stability of liposomal formulations entrapping loperamide HCl. (A) Release of loperamide HCl from nanoparticles in PBS pH 7.4 and 50% FCS at 37°C. The data represents the mean ± SEM as error bars of 3 independent experiments (P > 0.05; Mann-Whitney U test). (B and C) Particle size and polydispersity index over a period of 7 days of liposome formulation encapsulating loperamide HCl. The results are represented as mean ± SD of 3 independent experiments (P > 0.05, ANOVA).*

of loperamide HCl was not limited by the dialysis membrane. This confirms that loperamide HCl is able to run through the cellulose membrane tubing freely. In order to ensure stability of liposomes over time, experiments were conducted to monitor size and size distribution of the liposome formulation under storage conditions of 4°C in PBS pH 7.4 over 7 days. The size and polydispersity index of the liposome formulation are stable over this period (Fig. 2B and 2C). All liposomal formulations used in subsequent studies were stored at 4°C and used within 7 days of preparation.

Specificity of Immunoliposome Binding

To ensure the targeting efficacy of the liposome formulation was not affected following the incorporation of therapeutic molecules, the targeted liposomal system was assessed for specificity of binding and cellular uptake *in vitro* on primary high endothelial venule (HEV) cells cultured from rat lymph nodes. The different stages of growth of primary cultured HEV cells are depicted in Fig. 3A. At no stage was there more than one morphologically distinct type of cell present. To specifically identify HEV cells, immuno-labeling techniques were incorporated utilizing the endothelial cell marker OX-43. OX-43 labeling was particularly intense for the heavily vesiculated HEV cells in comparison to the proliferated bipolar morphological form (Fig. 3B).

Binding of ICAM-1-targeted immunoliposomes incorporating loperamide HCl was determined from using fluorometric detection. As shown in Fig. 4A, ICAM-1-targeted immunoliposomes incorporating loperamide HCL were capable of binding specifically to tumor necrosis factor-alpha (TNFα) activated endothelial cells in vitro, with 93.21% increase in binding in comparison to non-inflammatory conditions ($P < 0.01$; Mann-Whitney U test). The binding of liposomes and rabbit IgG immunoliposomes are significantly lower than that of loperamide HCl-encapsulated anti-ICAM-1 immunoliposomes to activated HEV cells ($P < 0.01$). The data also demonstrates the specificity of binding of loperamide HCl-encapsulated anti-ICAM-1 immunoliposomes to ICAM-1 expressing cells, as binding is significantly inhibited with preincubation with excess anti-ICAM-1 monoclonal antibodies ($P < 0.01$).

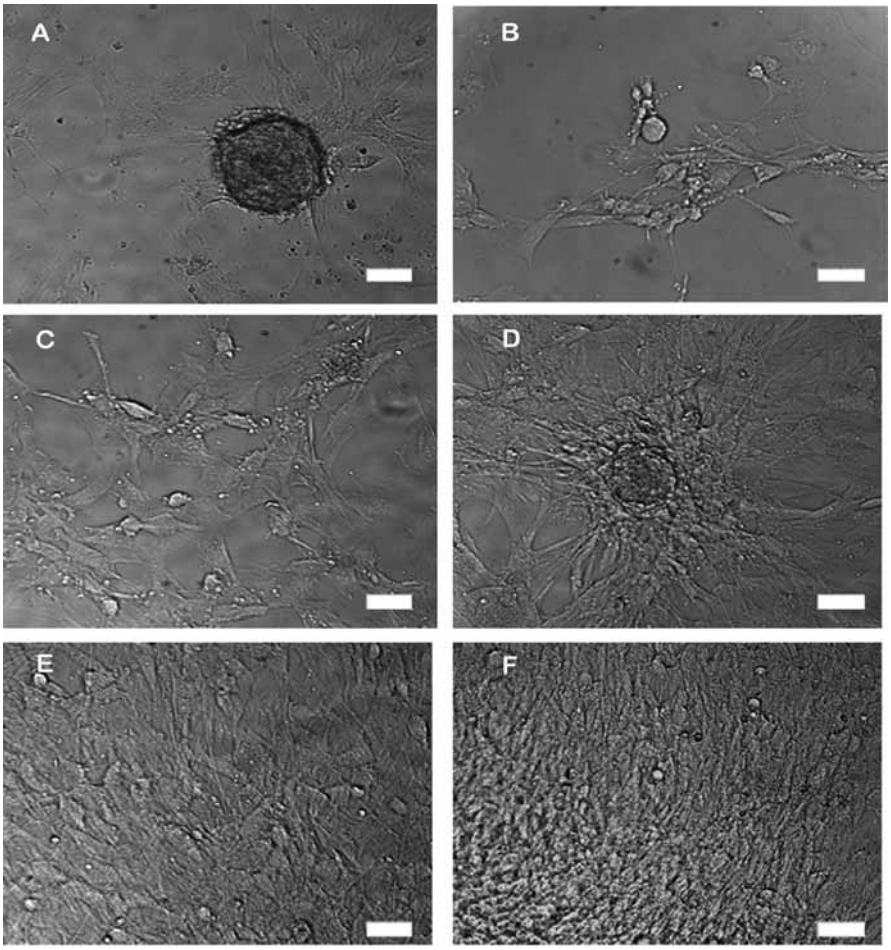

(A) A. Primary HEV culture after 2 days showing a flat, vesiculated cell. B and C: Primary HEV culture after 3 - 4 days showing cells adopting varying morphologies and proliferating. D: Primary HEV culture after 6 days showing cell growth in many orientations. E and F: Primary HEV culture after 10 days showing confluent bipolar cells aligned in a parallel array. Scale bar, 50 μm.

(B) Immunofluorescent staining of primary cultured HEV cells with FITC-conjugated mouse anti-rat OX-43 monoclonal antibody. A and C: Photomicrographs of primary HEV cell culture. B and D: Corresponding fluorescent micrographs showing OX-43 labeling of rat endothelial cells (green). The data is representative of 10 fields on 3 independent experiments. Scale bar, 50 μm.

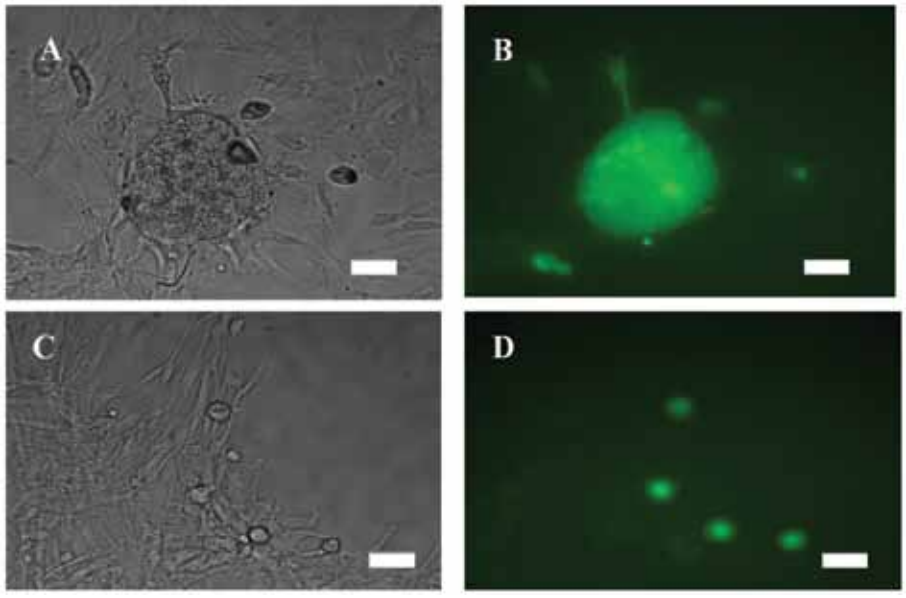

Fig. 3. *Phase contrast micrographs of HEV cells in culture.*

Degree of Cellular Uptake of Immunoliposomes

Cellular association of anti-ICAM-1 immunoliposomes with TNF-α-activated HEV cells was determined following an incubation time of 2 hours at 4°C and 5 hours at 37°C before analysis by fluorescence microplate spectroscopy. The degree of cellular uptake into vascular endothelial cells influences the proportion of nanoparticles able to undergo extravasation to the injured tissue and release of encapsulated opioids to the

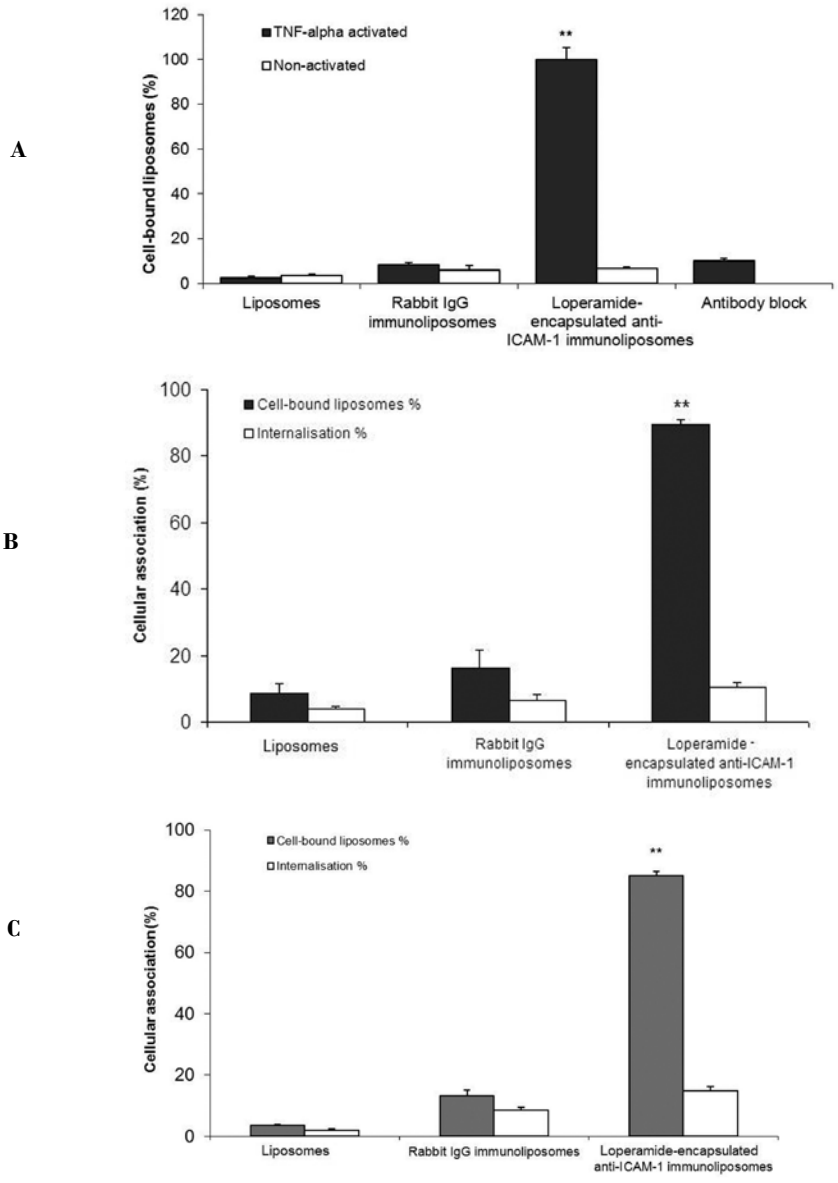

Fig. 4. *Fluorescence microplate spectroscopy data showing the cellular association of nanoparticles to HEV cells. (A) Specificity of binding to ICAM-1 on TNF-α activated and nonactivated HEV cells. Competitive inhibition of binding of loperamide HCl-encapsulated anti-ICAM-1 immunoliposomes following preincubation of TNF-α activated HEV cells with excess anti-ICAM-1 monoclonal antibodies is also shown. Liposomes were incubated at 3.38 mM for a time period of 2 hours at 4°C. (B and C) Internalization of nanoparticles by TNF-α activated HEV cells. Liposomes were incubated at (B) 5.79 mM or (C) 3.38 mM for 5 hours at 37°C. The results are represented as mean ± SEM of 9 independent experiments ($P < 0.01$; Mann Whitney U test).*

site of action. After 5 hours incubation at 37°C, minimal cellular internalization was detected for loperamide HCl-encapsulated anti-ICAM-1 immunoliposomes, rabbit IgG immunoliposomes, and liposomes at both 5.79 mM and 3.38 mM. Results following acid wash showed 89.49% ± 1.48% of cell-bound anti-ICAM-1 immunoliposomes compared to 16.07% ± 5.71% for rabbit IgG immunoliposomes, and 8.72% ± 2.87% for liposomes at 5.79 mM (Fig. 4B). Cellular association following liposome incubation at 3.38 mM resulted in similar findings (Fig. 4C). The data demonstrates that the cellular association of loperamide HCl-encapsulated anti-ICAM-1 immunoliposomes was due to binding to the surface of HEV cells, rather than cellular uptake ($P < 0.01$; Mann-Whitney U test). In addition, no significant uptake of liposomes occurred at 4°C across all groups.

Effects of the Intraplantar Injection of Complete Freund's Adjuvant (CFA)

Complete Freund's Adjuvant (CFA) induced a local inflammatory response characterized by unilateral oedema, hyperthermia, and hyperalgesia restricted to the inoculated hindpaw. Paw pressure thresholds (PPT) and paw volumes were measured before and after intraplantar CFA injection. The mean PPT value ± SEM (n = 36) before CFA injection was 162.3 ± 0.6 g for the inoculated hindpaw, and 161.6 ± 0.5 g for the contralateral hindpaw. The mean paw volume ± SEM as measured by displacement of the inoculated hindpaw was 1.026 ± 0.002 mL, and 1.043 ± 0.002 mL for the contralateral hindpaw. The mean PPT value ± SEM at day 5 following CFA injection of the inoculated hindpaw was 61.6 ± 0.3 g, and the mean paw volume as measured by displacement was 2.051 ± 0.004 mL. Analysis of the contralateral hindpaw was not significantly different pre- and post-CFA injection ($P > 0.05$), with a mean PPT ± SEM of 164.0 ± 0.5 g and mean paw volume ± SEM as measured by displacement of 1.036 ± 0.002 mL. The results demonstrate an approximate doubling in volume size of the inoculated hindpaw in comparison to the contralateral paw ($P < 0.0001$). Analysis of PPT of the ipsilateral inflamed paws post-CFA injection demonstrated a significant reduction in comparison to contralateral paws ($P < 0.0001$) and measured baseline values prior to CFA injection ($P < 0.0001$).

Time Course of the Antinociceptive Effect

The peak and duration of the antinociceptive effect of loperamide HCl-encapsulated anti-ICAM-1 immunoliposomes was evaluated over 48 hours. Figure 5A and 5B indicates that loperamide HCl-encapsulated anti-ICAM-1 immunoliposomes produced significant antinociception assessed by PPT on the ipsilateral (inflamed) paw of CFA-treated rats in comparison to the control groups ($P < 0.01$). In particular, the PPT of the loperamide HCL-encapsulated anti-ICAM-1 immunoliposome group was significantly higher at all time points from 1 hour to 48 hours in comparison to control groups. The results demonstrate a peak response at between 7 hours and 10 hours, which corresponds to a mean PPT value ± SEM (n = 6) of 127.5 ± 13.9 g and 124.2 ± 15.1 g, respectively ($P < 0.01$). Furthermore the results indicate a significant antinociceptive effect extending over the 48 hours time frame of the study, with a mean PPT value ± SEM of 98.6 ± 13.0 g at 24 hours ($P < 0.05$) and 90.3 ± 8.4 g at 48 hours ($P < 0.01$). Efficacy of the same loperamide HCl-encapsulated delivery system with and without the ICAM-1 targeted ligand attached to the surface of the liposomes clearly indicates the significant antinociceptive efficacy of the loperamide HCl-encapsulated delivery carrier with the ICAM-1 targeted ligand. Empty anti-ICAM-1 immunoliposomes did not demonstrate any antinociceptive activity, which indicates that the analgesic response was due to the release of loperamide HCl in the injured tissue. To examine opioid receptor dependency of the antinociceptive actions, the peripheral opioid receptor antagonist, naloxone methiodide, was administered via intraplantar injection 15 minutes prior to loperamide-encapsulated anti-ICAM-1 immunoliposomes. Naloxone methiodide was able to significantly reverse the antinociceptive effect of the loperamide-encapsulated targeted nanoparticles over the first 4 hours ($P < 0.01$), which corresponds to its duration of action. As the naloxone methiodide wears off, we can see a significant antinociceptive response at the 7 hours ($P < 0.01$) to 48 hours ($P < 0.001$) time points, which is likely to indicate a combination of exogenous loperamide-HCl and endogenous opioid activity. The mean PPT throughout the 48-hour period was not significantly different between the other control groups, which indicates that loperamide HCl alone and the drug vehicle itself does not have any antinociceptive effect when administered systemically ($P > 0.05$). Paw pressure thresholds of the contralateral (non-inflamed) paw of control and loperamide HCl treatment groups were not significantly different compared to each other across all time points over the 48-hour period (Fig. 5A).

Time Course of the Anti-inflammatory Effect

Paw volume was used to assess inflammation in

A

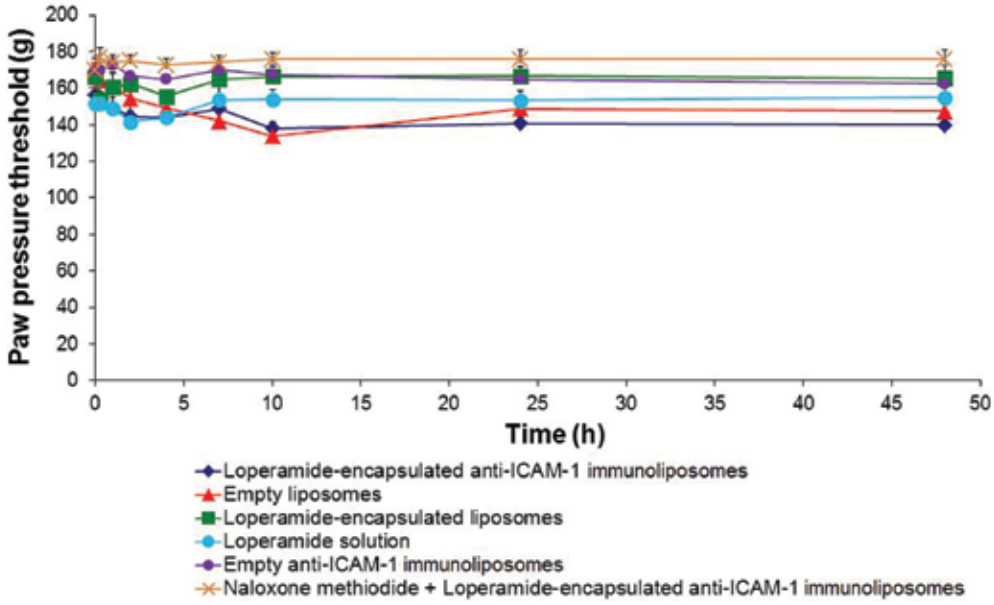

B

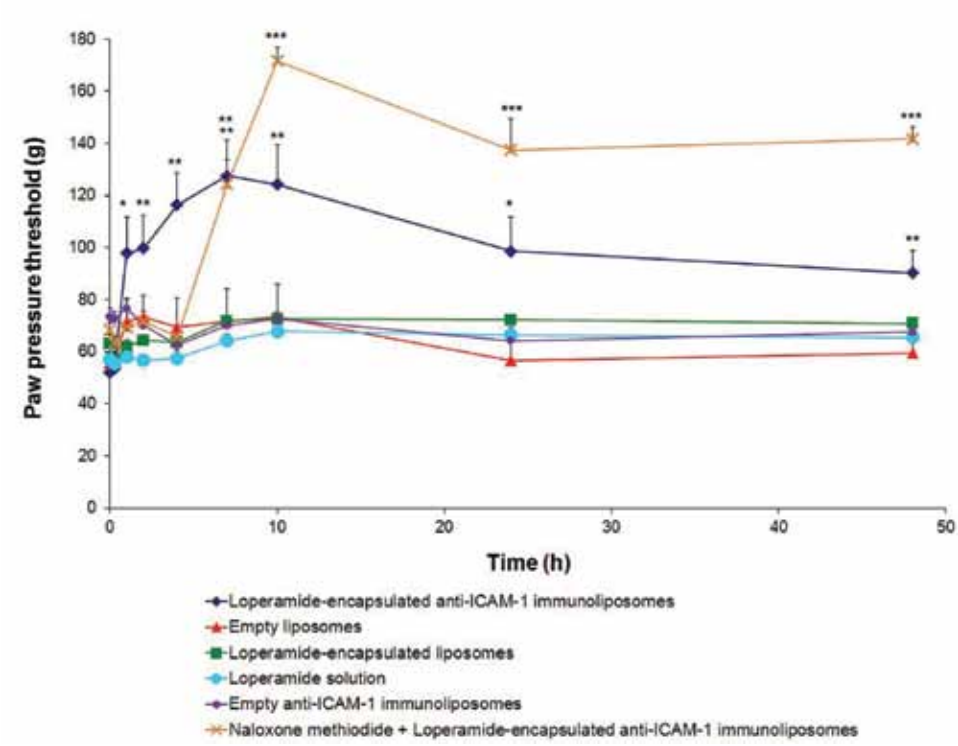

Fig. 5. *Time course of the antinociceptive effects of loperamide HCl-encapsulated anti-ICAM-1 immunoliposomes and control formulations in Complete Freund's Adjuvant (CFA) treated animals. (A) Data is presented in terms of paw pressure thresholds (PPT) of the contralateral (non-inflamed) paw. (B) Data is presented in terms of paw pressure threshold (PPT) of the ipsilateral (inflamed) paw. Each point represents the mean PPT value ± SEM of 6 animals. Mann-Whitney U test was used to assess intergroup differences (*P < 0.05, **P < 0.01, ***P < 0.001).*

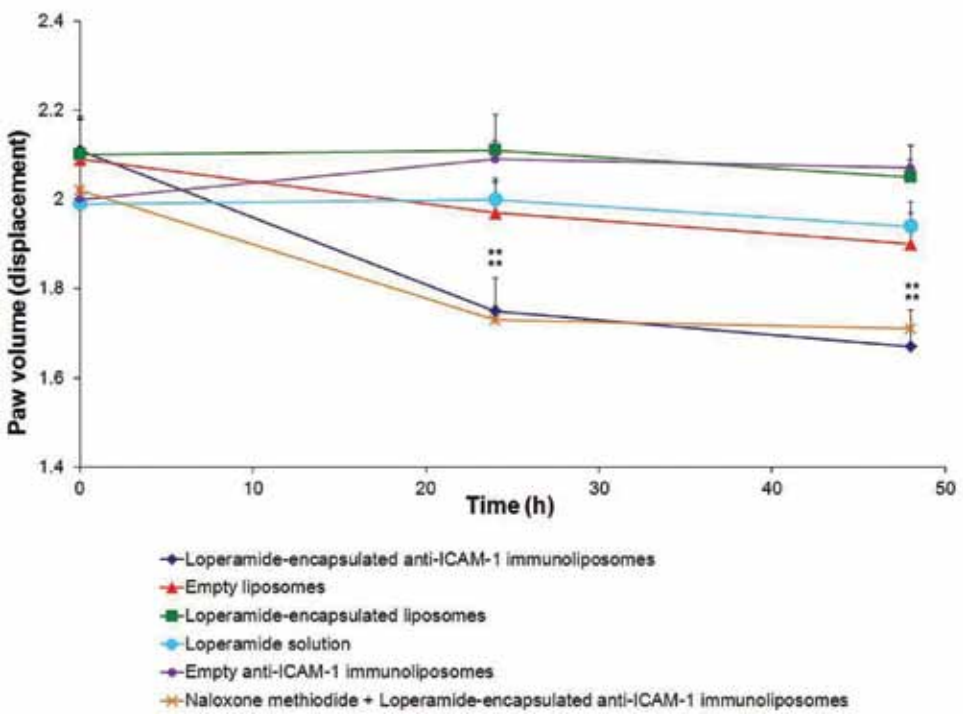

Fig. 6. *Time course of the anti-inflammatory effects of loperamide HCl-encapsulated anti- ICAM-1 immunoliposomes and control formulations in Complete Freund's Adjuvant (CFA) treated animals. Data is presented in terms of paw volume of the ipsilateral (inflamed) paw. Each point represents the mean displacement volume ± SEM of 6 animals. ANOVA was used to assess differences relative to baseline (**$P < 0.01$).*

terms of displacement at baseline, 24 hours, and 48 hours. No significant difference was seen for paw volume of the contralateral paws of all the study groups pre- and post-CFA injection ($P > 0.05$). The ipsilateral paws of the study groups at day 5 post-CFA injection have an approximate doubling in volume size compared to the contralateral paws at baseline ($P < 0.0001$, Mann- Whitney U test, n = 36), which demonstrates a localized inflammatory response. At 24 hours and 48 hours, the loperamide HCl-encapsulated anti-ICAM-1 immunoliposome group demonstrated a significant decrease in paw volume with a mean displacement ± SEM (n = 6) of 1.753 ± 0.074 mL and 1.674 ± 0.081 mL, respectively, in comparison to mean baseline displacement of 2.110 ± 0.070 mL ($P < 0.01$, ANOVA, n = 6) (Fig. 6). The naloxone methiodide + loperamide-encapsulated anti-ICAM-1 immunoliposome group also demonstrated an anti-inflammatory effect at 24 hours and 48 hours ($P < 0.01$, ANOVA, n = 6). All other control groups showed no significant difference at 24 hours and 48 hours in comparison to baseline values ($P > 0.05$, ANOVA).

Effect of ICAM-1 Targeting on Tissue Distribution of Liposomes

Tissue biodistribution of the loperamide HCl-encapsulated anti-ICAM-1 immunoliposomes was assessed following intravenous administration in CFA-induced paw inflammation in rats. Loperamide HCl-encapsulated liposomes acted as the control group. Studies were performed 5 days post-CFA injection, which corresponded to peak inflammatory response. Rats were sacrificed 7 hours after liposome injection, and paw tissues and other indicated organs (brain, liver, and kidneys) were removed for processing of radioactivity using liquid scintillation counting (LSC). Tissue distribution was evaluated at 7 hours post-liposome injection as peak antinociceptive efficacy of loperamide HCl-encapsulated anti-ICAM-1 immunoliposomes was demonstrated at

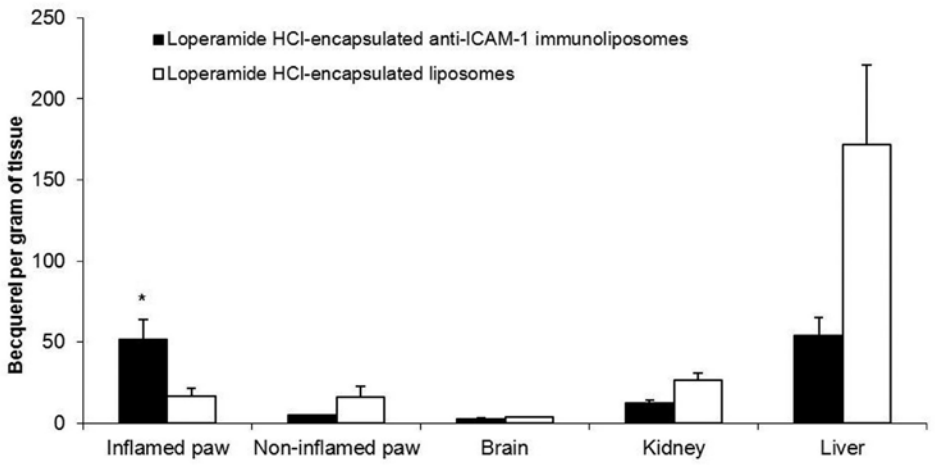

Fig. 7. *Biodistribution of [^{3}H]-CHE radiolabelled loperamide HCl-encapsulated anti-ICAM-1 immunoliposomes and loperamide HCl-encapsulated liposomes in Complete Freund's Adjuvant (CFA)-induced paw inflammation in rats. Rats were sacrificed 7 hours after intravenous injection of 200 μL of liposome suspension (equivalent to 7.41 x 10^4 Bq). Each point represents the mean Bq per gram of tissue ± SEM of 4 animals. Mann-Whitney U test was used to assess intergroup differences (*P < 0.05).*

this time point in *in vivo* efficacy studies. The dose of radiolabelled liposomes injected intravenously per rat was equivalent to 7.41 x 10^4 Bq of [^{3}H]-CHE.

Figure 7 shows the biodistribution of radiolabelled loperamide HCl-encapsulated anti-ICAM-1 immunoliposomes and radiolabelled loperamide HCl-encapsulated liposomes in CFA-induced paw inflammation in rats. Conjugation of anti-ICAM-1 monoclonal antibodies to the surface of long-circulating immunoliposomes increased the uptake into the inflamed paw tissue by 3-fold at 7 hours in comparison to liposomes without the targeting ligand ($P < 0.05$, Mann-Whitney U test). The uptake of loperamide HCl-encapsulated ICAM-1 targeted immunoliposomes into the inflamed paw tissue was 10.8-fold higher than uptake into the non-inflamed paw tissue ($P < 0.05$). Minimal uptake into the brain was detected with no significant difference for both the ICAM-1 targeted immunoliposome and control formulation ($P > 0.05$), further demonstrating a peripheral opioid receptor-mediated effect. Correspondingly, a 2-fold and 3-fold decrease in uptake of anti-ICAM-1 targeted immunoliposomes was detected in both the kidneys and liver, respectively, in comparison with the control ($P < 0.05$), which indicates that the targeted nanoparticles are not readily taken up by the reticuloendothelial system (RES) and hence are available for prolonged circulation and controlled release. Conversely, the control liposomes showed a large variability in uptake into the liver in comparison to the ICAM-1 targeted immunoliposomes. Comparison of the biodistribution into non-inflamed paw tissue showed a significant uptake of control liposomes in comparison with the loperamide HCl-encapsulated anti-ICAM-1 immunoliposomes ($P < 0.05$). No significant difference in distribution to inflamed and non- inflamed paw tissue was detected for the loperamide HCl-encapsulated liposome group ($P > 0.05$).

Discussion

We have engineered targeted nanoparticles that are able to mimic the actions of endogenous opioid-containing immune cells in response to tissue injury, to provide significant and prolonged analgesic and anti-inflammatory effects. Incorporation of ICAM-1 targeting ligands to the surface of the liposomes increases localization to peripheral inflammatory tissue, thereby increasing the therapeutic potency of the targeted nanoparticles. ICAM-1 is a cell adhesion molecule that is upregulated and functionally involved in inflammation (7,23). It is localized to both the apical and basolateral surface of endothelial cells and does not undergo significant internalization, making it ideally positioned to facilitate immune cell recruitment and transendothelial migration (24). Furthermore, ICAM-1 plays an important role in peripheral analgesia at both the endothelial (25,26) and immune cell-neuronal level (6). We have

demonstrated specific binding and minimal cellular uptake of the targeted nanoparticles to vascular endothelial cells preincubated with the inflammatory cytokine TNF-α, which allows extravasation of the targeted nanoparticles across the endothelial barrier directed by ICAM-1 on the surface of endothelial cells at sites of inflammation and the subsequent release of encapsulated opioids in close vicinity to upregulated peripheral opioid receptors in injured tissue (1). This peripheral analgesic pathway has yet to be targeted in pharmaceutical formulation and clinical pain management.

Incorporation of loperamide HCl into ICAM-1 targeted immunoliposomes allows the intravenous use of this antidiarrhoeal agent as a peripherally selective analgesic, which has not been achieved prior to this study. The antinociceptive effects of loperamide HCl have previously been observed in various models of chemical-induced inflammatory pain and constant thermal hyperalgesia after local (11,14,27) and systemic (subcutaneous) (13,14) routes of administration. Binding studies have demonstrated that loperamide HCl has a strong affinity and high selectivity for mu-opioid receptors (9,11,28), however it does not have analgesic effects when administered orally or intravenously due to its physicochemical properties (1,10-14). Its exclusion from the CNS is apparently due to its active removal by the multi-drug resistance transporter, its high affinity to lipid membranes, and its ability to decrease surface tension (11,14,27,28). This contributes to its accumulation in membranes and subsequent lack of systemic absorption (27,28). After intravenous or oral application loperamide HCl becomes trapped in the liver, kidneys, and lungs, or stomach and intestines, respectively (27). Opioid-like antinociception in rodents after intravenous injection of the free drug occurs only at almost lethal doses (9). Encapsulation of loperamide HCl within long circulating ICAM-1-targeted immunoliposomes allows both prolonged circulation and active targeting to sites of inflammation, thereby allowing a lower dose to be administered systemically.

Under physiological conditions, solute leakage depends not only on the intrinsic membrane permeability but also its interaction with components of the biological fluid, which strongly affect liposome clearance (29). In vitro stability studies of the DSPC with cholesterol liposome formulation entrapping loperamide HCl have demonstrated highly stable vesicles upon dilution in an aqueous phase (PBS pH 7.4) and in serum (50% FCS). The results suggest that the targeted nanoparticles will be suitable for use in administration of loperamide HCl to sites of high dilution such as following intravenous administration. The minimal release of loperamide HCl from DSPC with cholesterol liposome formulations at 37°C may be attributed to the more stable outer surface of the liposome formulation, thereby keeping loperamide HCl entrapped in the lipid bilayer. Stability against leakage has been achieved using phospholipids (e.g., DSPC) that remain in the solid phase at physiological temperatures. Incorporating cholesterol generally enhances bilayer stability against leakage by minimising lipid exchange (30). The ICAM-1 targeted immunoliposomes in this study have both a mean particle size of 286 ± 7.9 nm and a neutral net charge, conferring long-circulation half-lives. If the recognition of liposomes as a foreign body by the immune system can be circumvented, these vesicles could circulate in the bloodstream longer to interact with their target and even extravasate through leaky or fenestrated endothelium.

Peripheral inflammation enhances the effects of exogenously administered opioid agonists (1). We are the first to demonstrate that targeting the peripheral opioid system by mimicking opioid-containing immune cells has significant analgesic and anti-inflammatory effects. Loperamide HCl-encapsulated anti-ICAM-1 immunoliposomes produced significant antinociception over the 48 hour time course studied following intravenous administration, by specific localization of the targeted carrier to peripheral inflammatory tissue. This allows the release of loperamide HCl in close vicinity to the upregulated peripheral opioid receptors in inflammation to provide site-directed antinociception (6). Evaluation of paw pressure thresholds (PPT) of the loperamide HCl-encapsulated anti-ICAM-1 immunoliposome group demonstrated a peak antinociceptive effect between 7 hours to 10 hours, and a significant prolonged antinociceptive response as assessed over 48 hours. The controlled release effect may be due to the use of saturated phospholipids with high lipid phase transition temperatures (Tm), thus conferring both prolonged circulation (30,31) and specific release at sites of hyperthermia (32,33), which is a characteristic of inflammation.

It is unlikely that anti-ICAM-1 monoclonal antibodies on the surface of the targeted liposomes blocked the function of ICAM-1 on the apical surface of vascular endothelial cells, and hindered the extravasation of immune cells containing pro-inflammatory factors to cause the analgesic and anti-inflammatory effects. This is supported by the lack of analgesic and anti-inflammatory activity by empty anti-ICAM-1 immunoliposomes and

loperamide HCl-encapsulated liposomes, in comparison to the loperamide-encapsulated targeted nanoparticles. Administration of anti-ICAM-1 monoclonal antibodies at this concentration (25 μg) has not been previously demonstrated to have analgesic or anti-inflammatory effects (34-36). More specifically when monoclonal antibodies targeting cell adhesion molecules are conjugated to liposomes, the carrier system either undergoes binding and extravasation, or cellular internalisation in inflammation (37). The potential to inhibit leukocyte adhesion to the endothelium and thus extravasation into the inflammatory tissue only exists when administering high concentrations of free anti-ICAM-1 monoclonal antibodies (34-36). For example, Ioculano et al (34) assayed the pathophysiological role of ICAM-1 in a model of ischaemia reperfusion in the rat. Intravenous administration of anti-rat ICAM-1 monoclonal antibodies at a dose of 1 mg/kg, which equated to 250 – 360 μg, prior to occlusion of the left main coronary artery, significantly decreased leukocyte accumulation. Our data suggest that the targeted nanoparticles may escape from the gaps between adjacent endothelial cells and openings at the vessel termini during inflammation by passive convective transport and/or ligand-directed targeting (37,38).

This phenomenon of disease-site targeting is believed to play a major role in the enhanced efficacy observed for a variety of drugs when formulated inside lipid vesicles (39- 41). More importantly, Tosi et al (42) investigated the in vivo antinociceptive efficacy of peptide-derivatised nanoparticles loaded with loperamide HCl for delivery to the CNS, and reported a peak percentage of maximum possible effect (% MPE) of 60% at 4 hours and a significant sustained release effect for 6 hours after tail vein injection of a dose equivalent of 0.7 mg of loperamide HCl in Wistar rats. The investigators reported that this long-lasting effect had not been shown before, with previous studies in the literature showing maximum antinociceptive effect at the same dose of loperamide HCl of between 15 minutes and 1 hour, before a rapid decrease in antinociceptive efficacy (10,43). This is in contrast to our results, which shows a peak antinociceptive effect between 7 hours to 10 hours, and a significant and prolonged antinociceptive effect over 48 hours following the intravenous administration of long circulating loperamide HCl-encapsulated anti-ICAM-1 immunoliposomes, with a dose equivalent of 0.8 mg of loperamide HCl. In addition the antinociceptive activity of the loperamide HCl-encapsulated targeted immunoliposomes was able to be reversed with naloxone methiodide, which suggest an opioid-receptor dependent analgesic effect. Naloxone methiodide has a relatively short duration of action, which our data confirms, showing that when administered via intraplantar injection, its effects last for approximately 4 hours.

There is growing evidence that opioid peptides are also potent modulators of cellular immune response, which can enhance or inhibit immune functions (1,44-46). The analysis of paw volume following administration of loperamide HCl-encapsulated anti-ICAM-1 immunoliposomes showed a significant decrease at 24 hours and 48 hours in comparison to baseline displacement values, even when naloxone methiodide was administered beforehand. As the duration of action of naloxone methiodide is relatively short, we did not expect this to affect the anti-inflammatory response of the targeted nanoparticles as anti-inflammatory action is never immediate. This is in contrast to the control groups, which did not demonstrate a significant change in paw volume assessed over 48 hours. It is plausible that the anti-inflammatory effect observed following administration of loperamide HCl-encapsulated anti-ICAM-1 immunoliposomes is a result of opioid mediated inhibition of leukocyte recruitment to inflamed tissue (47-51), or partly due to opioid mediated detachment of immune cells from sensory neurons (6) – in this way preventing the release of cytokines and other inflammatory factors into the injured tissue. However, empty anti-ICAM-1 immunoliposomes did not demonstrate any anti-inflammatory activity, making the former mechanism less likely. We have previously shown that opioids can interfere with the direct cell adhesion between immune cells and neurons via an opioid receptor dependent mechanism, which may result in dissociation and migration of leukocytes back to regional lymph nodes (6). This is in contrast to morphine which has been reported to have anti-oedema effects in rats with carrageenan-induced inflammation of the paw (52), potentially as a result of down-regulation of adhesion molecules on endothelial cells necessary for leukocyte transmigration, via stimulation of nitric oxide production (48). Our results highlight a novel anti-inflammatory role for peripheral opioid targeting with loperamide HCl.

Biodistribution studies of loperamide HCl-encapsulated ICAM-1 targeted immunoliposomes showed predominant targeting of the nanoparticles into peripheral inflamed tissue, with minimal accumulation in non-inflamed paw tissue and the brain. This confirms that the antinociceptive effect observed following intravenous administration of loperamide HCl-encap-

sulated ICAM-1 targeted immunoliposomes was due to peripheral opioid receptor targeting, rather than a central opioid-mediated effect. As further support, the antinociceptive effect of the opioid-encapsulated targeted nanoparticles was able to be blocked with naloxone methiodide. Loperamide HCl does not elicit an effect on the CNS when administered as the free drug form as it is a substrate for the multi-drug resistance transporter (11,14). ICAM-1 is also not normally upregulated in the blood-brain barrier (BBB) or CNS (53,54). In addition, the significant anti-inflammatory effect following intravenous administration of loperamide HCl-encapsulated anti-ICAM-1 immunoliposomes suggests a more localized response at the peripheral inflammatory site rather than distribution into the CNS. The biodistribution data also shows limited uptake of the targeted nanoparticles by the reticuloendothelial system (RES) (e.g., liver, kidneys), which allows prolonged systemic circulation and controlled release. This is of importance as liposomes with entrapped materials have previously been rapidly cleared due to opsonisation of plasma components and uptake by fixed macrophages of the reticuloendothelial system (RES), thereby limiting their prospects as an in vivo delivery system for transporting drugs to sites of disease beyond the RES.

Conclusion

The interaction of the immune system and nervous system in peripheral pain control is of significant clinical relevance. We have engineered targeted nanoparticles to mimic this interaction that takes place within injured tissue to provide peripherally selective analgesic and anti-inflammatory effects, using loperamide HCl. Although the nociceptive and anti-inflammatory testing methods have been well established in the literature, future studies may consider using additional methods (e.g., assessing thermal hyperalgesia, or using an electronic von Frey anesthesiometer to assess mechanical allodynia). It will be of much interest to elucidate the mechanism of the anti-inflammatory effect of loperamide HCl-encapsulated anti-ICAM-1 immunoliposomes. We are currently assessing the analgesic and anti-inflammatory effects of the targeted nanoparticles in chronic pain models. These results are encouraging in the progress towards novel, effective, and safe analgesic and anti-inflammatory therapies that avoid the serious central side effects of opioids and those of nonsteroidal and steroidal anti-inflammatory drugs (55-57). This long-acting peripheral formulation may potentially be used in the management of acute painful inflammatory conditions (e.g., postoperative pain) and chronic painful inflammatory conditions (e.g., arthritis and neuropathic pain). This study has implications on understanding the process of inflammatory diseases affecting the peripheral system, and the use of opioids as peripheral analgesics and anti-inflammatories using drug delivery and targeting. The potential also exists for the modification of these targeted nanoparticles with other therapeutic compounds for use in other biomedical applications.

References

1. Hua S, Cabot PJ. Mechanisms of peripheral immune-cell-mediated analgesia in inflammation: Clinical and therapeutic implications. *Trends in Pharmacological Sciences* 2010; 31:427-433.
2. Moalem G, Tracey DJ. Immune and inflammatory mechanisms in neuropathic pain.*Brain Res Rev* 2006; 51:240-264.
3. Machelska H, Schopohl JK, Mousa SA, Labuz D, Schafer M, Stein C. Different mechanisms of intrinsic pain inhibition in early and late inflammation. *J Neuroimmunol* 2003; 141:30-39.
4. Cabot PJ, Carter L, Schafer M, Stein C. Methionine-enkephalin-and Dynorphin A- release from immune cells and control of inflammatory pain. *Pain* 2001; 93:207-212.
5. Cabot PJ, Carter L, Gaiddon C, Zhang Q, Schafer M, Loeffler JP, Stein C. Immune cell-derived beta-endorphin. Production, release, and control of inflammatory pain in rats. *J Clin Invest* 1997; 100:142-148.
6. Hua S, Hermanussen S, Tang L, Monteith GR, Cabot PJ. The neural cell adhesion molecule antibody blocks cold water swim stress-induced analgesia and cell adhesion between lymphocytes and cultured dorsal root ganglion neurons. *Anesth & Analg* 2006; 103:1558-1564.
7. Hubbard AK, Rothlein R. Intercellular adhesion molecule-1 (ICAM-1) expression and cell signaling cascades. *Free Radic Biol Med* 2000; 28:1379-1386.
8. Gilman AG, Rall TW, Nies AS, Taylor P. *The Pharmacological Basis of Therapeutics: Opioid Analgesics and Antagonists.* McGraw-Hill, New York, 1993, pp 485-521.
9. Wuster M, Herz A. Opiate agonist action of antidiarrheal agents in vitro and in vivo- findings in support for selective action. *Naunyn-Schmiedeberg's Arch Pharmacol* 1978; 301:187-194.
10. Alyautdin RN, Petrov VE, Langer K, Berthold A, Kharkevich DA, Kreuter J. Delivery of loperamide across the blood-brain barrier with polysorbate 80-coated polybutylcyanoacrylate nanoparticles. *Pharmaceut Res* 1997; 14:325-328.
11. DeHaven-Hudkins DL, Burgos LC, Cassel JA, Daubert JD, DeHaven RN, Mansson E, Nagasaka H, Yu G, Yaksh T. Loperamide (ADL 2-1294), an opioid antihyperalgesic agent with peripheral selectivity. *J Pharmacol Exp Ther* 1999; 289:494-502.
12. Hagiwara K, Nakagawasai O, Murata A, Yamadera F, Miyoshi I, Tan-No K, Tadano T, Yanagisawa T, Iijima T, Murakami M. Analgesic action of loperamide, an opioid agonist, and its blocking action on voltage-dependent Ca2+ channels. *Neurosci Res* 2003; 46:493-497.

13. Menendez L, Lastra A, Meana A, Hidalgo A, Baamonde A. Analgesic effects of loperamide in bone cancer pain in mice. *Pharmacol Biochem Behav* 2005; 81:114- 121.
14. Sevostianova N, Danysz W, Bespalov AY. Analgesic effects of morphine and loperamide in the rat formalin test: Interactions with NMDA receptor antagonists. *Eur J Pharmacol* 2005; 525:83-90.
15. Stein C, Lang LJ. Peripheral mechanisms of opioid analgesia. *Curr Opin Pharmacol* 2009; 9:3-8.
16. Stein C, Schafer M, Machelska H. Attacking pain at its source: New perspectives on opioids. *Nat Med* 2003; 9:1003-1008.
17. Hua S, Chang HI, Davies NM, Cabot PJ. Targeting of ICAM-1-directed immunoliposomes specifically to activated endothelial cells with low cellular uptake: liposomes. *J Liposome Res* 2011; 21:95-105.
18. Ager A. Isolation and culture of high endothelial cells from rat lymph nodes. *J Cell Sci* 1987; 87:133-144.
19. Kessner S, Krause A, Rothe U, Bendas G. Investigation of the cellular uptake of E-Selectin-targeted immunoliposomes by activated human endothelial cells. *Biochim Biophys Acta* 2001; 1514:177-190.
20. Voinea M, Manduteanu I, Dragomir E, Capraru M, Simionescu M. Immunoliposomes directed toward VCAM-1 interact specifically with activated endothelial cells--a potential tool for specific drug delivery. *Pharm Res* 2005; 22:1906-1917.
21. Everts M, Koning GA, Kok RJ, Asgeirsdottir SA, Vestweber D, Meijer DK, Storm G, Molema G. In vitro cellular handling and in vivo targeting of E-selectin-directed immunoconjugates and immunoliposomes used for drug delivery to inflamed endothelium. *Pharm Res* 2003; 20:64-72.
22. PerkinElmer. 2007. LSC in Practice: SOLVABLE-- solubilization protocols for whole human blood, PAGE gels and glass fiber filters. In: *Application note*: PerkinElmer.
23. Koning GA, Schiffelers RM, Storm G. Endothelial cells at inflammatory sites as target for therapeutic intervention. *Endothelium* 2002; 9:161-171.
24. Almenar-Queralt A, Duperray A, Miles LA, Felez J, Altieri DC. Apical topography and modulation of ICAM-1 expression on activated endothelium. *Am J Pathol* 1995; 147:1278-1288.
25. Gahmberg C. Leukocyte adhesion: CD11/CD18 integrins and intercellular adhesion molecules. *Curr Opin Cell Biol* 1997; 9:643-650.
26. Rittner HL, Stein C. Involvement of cytokines, chemokines and adhesion molecules in opioid analgesia. *Eur J Pain* 2005; 9:109-112.
27. Stein C, Machelska H, Schafer M. Peripheral analgesic and antiinflammatory effects of opioids. *Z Rheumatol* 2001; 60:416-424.
28. Heel RC, Brogden RN, Speight TM, Avery GS. Loperamide: A review of its pharmacological properties and therapeutic efficacy in diarrhoea. *Drugs* 1978; 15:33-52.
29. Ishida T, Harashima H, Kiwada H. Interactions of liposomes with cells in vitro and in vivo: Opsonins and receptors. *Curr Drug Metab* 2001; 2:397-409.
30. Anderson M, Omri A. The effect of different lipid components on the in vitro stability and release kinetics of liposome formulations. *Drug Deliv* 2004; 11:33-39.
31. Ono A, Takeuchi K, Sukenari A, Suzuki T, Adachi I, Ueno M. Reconsideration of drug release from temperature-sensitive liposomes. *Biol Pharm Bull* 2002; 25:97-101.
32. Kong G, Anyarambhatla G, Petros WP, Braun RD, Colvin OM, Needham D, Dewhirst MW. Efficacy of liposomes and hyperthermia in a human tumor xenograft model: Importance of triggered drug release. *Cancer Res* 2000; 60:6950-6957.
33. Lindner LH, Eichhorn ME, Eibl H, Teichert N, Schmitt-Sody M, Issels RD, Dellian M. Novel temperature-sensitive liposomes with prolonged circulation time. *Clin Cancer Res* 2004; 10:2168-2178.
34. Ioculano M, Squadrito F, Altavilla D, Canale P, Squadrito G, Campo GM, Saitta A, Caputi AP. Antibodies against intercellular adhesion molecule 1 protect against myocardial ischaemia-reperfusion injury in rat. *Eur J Pharmacol* 1994; 264:143-149.
35. Kavanaugh AF, Davis LS, Jain RI, Nichols LA, Norris SH, Lipsky PE. A phase I/II open label study of the safety and efficacy of an anti-ICAM-1 (intercellular adhesion molecule-1; CD54) monoclonal antibody in early rheumatoid arthritis. *J Rheumatol* 1996; 23:1338-1344.
36. Rothlein R, Mainolfi EA, Kishimoto TK. Treatment of inflamation with anti -ICAM-1. *Res Immunol* 1993; 144:735-762.
37. Metselaar JM, Storm G. Liposomes in the treatment of inflammatory disorders. *Expert Opin Drug Deliv* 2005; 2:465-476.
38. Antohe F, Lin L, Kao GY, Poznansky MJ, Allen TM. Transendothelial movement of liposomes in vitro mediated by cancer cells, neutrophils or histamine. *J Liposome Res* 2004; 14:1-25.
39. Bendas G. Immunoliposomes: A promising approach to targeting cancer therapy. *BioDrugs* 2001; 15:215-224.
40. Maruyama K. PEG-immunoliposome. *Biosci Rep* 2002; 22:251-266.
41. Willis M, Forssen E. Ligand-targeted liposomes. *Adv Drug Deliv Rev* 1998; 29:249- 271.
42. Tosi G, Costantino L, Rivasi F, Ruozi B, Leo E, Vergoni AV, Tacchi R, Bertolini A, Vandelli MA, Forni F. Targeting the central nervous system: In vivo experiments with peptide-derivatized nanoparticles loaded with Loperamide and Rhodamine-123. *J Control Release* 2007; 122:1-9.
43. Michaelis K, Hoffmann MM, Dreis S, Herbert E, Alyautdin RN, Michaelis M, Kreuter J, Langer K. Covalent linkage of apolipoprotein E to albumin nanoparticles strongly enhances drug transport into the brain. *J Pharm Exp Ther* 2006; 317:1246- 1253.
44. Brown SL, Van Epps DE. Suppression of T lymphocyte chemotactic factor production by the opioid peptides beta-endorphin and met-enkephalin. *J Immunol* 1985; 134:3384-3390.
45. van Epps DE, Saland L. Beta-endorphin and met-enkephalin stimulate human peripheral blood mononuclear cell chemotaxis. *J Immunol* 1984; 132:3046-3053.
46. Van Epps DE, Saland L, Taylor C, Williams RC, Jr. In vitro and in vivo effects of beta-endorphin and met-enkephalin on leukocyte locomotion. *Prog Brain Res* 1983; 59:361-374.
47. Fischer EG, Stingl A, Kirkpatrick CJ. Opioid influence on the adherence of granulocytes to human umbilical vein endothelial cells in vitro. *Cell Biol Int Rep* 1990; 14:797-804.
48. Ni X, Gritman KR, Eisenstein TK, Adler MW, Arfors KE, Tuma RF. Morphine attenuates leukocyte/endothelial interactions. *Microvasc Res* 2000; 60:121-130.
49. Pasnik J, Tchorzewski H, Baj Z, Luciak M, Tchorzewski M. Priming effect of met- enkephalin and beta-endorphin on chemiluminescence, chemotaxis and CD11b molecule expression on human neutrophils in vitro. *Immunol Lett* 1999; 67:77-83.

50. Pello OM, Duthey B, Garcia-Bernal D, Rodriguez-Frade JM, Stein JV, Teixido J, Martinez C, Mellado M. Opioids trigger alpha 5 beta 1 integrin-mediated monocyte adhesion. *J Immunol* 2006; 176:1675-1685.

51. Van Epps DE, Kutvirt SL. Modulation of human neutrophil adherence by beta-endorphin and met-enkephalin. *J Neuroimmunol* 1987; 15:219-228.

52. Planas E, Sanchez S, Rodriguez L, Pol O, Puig MM. Antinociceptive/anti-edema effects of liposomal morphine during acute inflammation of the rat paw. *Pharmacology* 2000; 60:121-127.

53. Bullard DC, Hu X, Schoeb TR, Collins RG, Beaudet AL, Barnum SR. Intercellular adhesion molecule-1 expression is required on multiple cell types for the development of experimental autoimmune encephalomyelitis. *J Immunol* 2007; 178:851-857.

54. Carlos TM, Clark RS, Franicola-Higgins D, Schiding JK, Kochanek PM. Expression of endothelial adhesion molecules and recruitment of neutrophils after traumatic brain injury in rats. *J Leukoc Biol* 1997; 61:279-285.

55. Rittner HL, Brack A. Leukocytes as mediators of pain and analgesia. *Curr Rheumatol Rep* 2007; 9:503-510.

56. Warner TD, Mitchell JA. COX-2 selectivity alone does not define the cardiovascular risks associated with non-steroidal anti-inflammatory drugs. *Lancet* 2008; 371:270- 273.

57. Stein C, Clark JD, Oh U, Vasko MR, Wilcox GL, Overland AC, Vanderah TW, Spencer RH. Peripheral mechanisms of pain and analgesia. *Brain Res Rev* 2009; 60:90-113.